2012

Engineered Carbon-Nanotubes Based Composite Material for RF Applications

Emmanuel Decrossas

Mahmoud EL Sabbagh
Syracuse University, msabbagh@syr.edu

Samir M. El-Ghazaly

Victor Fouad Hanna

Recommended Citation

E. Decrossas, M. A. El Sabbagh, S. M. El-Ghazaly, and V. F. Hanna, "Engineered Carbon-Nanotubes-Based Composite Material for RF Applications," Ieee Transactions on Electromagnetic Compatibility, vol. 54, pp. 52-59, Feb 2012.

Engineered Carbon-Nanotubes Based Composite Material for RF Applications

Emmanuel Decrossas[1], Mahmoud A. EL Sabbagh[2], Samir M. El-Ghazaly[1] and Victor Fouad Hanna[3]

[1] Dept. of Electrical Engineering, University of Arkansas, Fayetteville, AR, 72701, USA
edecrossas@ieee.org, elghazal@uark.edu

[2] Dept. of Electrical Engineering and Computer Science, Syracuse University, NY, 13244, USA
msabbagh@ieee.org

[3] Université Pierre et Marie Curie - Paris 6, EA 2385, L2E, F-75252, Paris, France
victor.fouad_hanna@upmc.fr

***Abstract* — Electrical properties of nano-composite materials are extracted to investigate the possibility to engineer novel material for microwave applications. A measurement setup is developed to characterize material in a powder form. The developed measurement technique is applied on nano-particles of alumina, carbon nanotubes (CNTs), and composite mixture of carbon nanotubes and alumina. The effect of packing density on dielectric constant and loss tangent is thoroughly characterized experimentally. The obtained results show that the real part of effective permittivity may be considerably enhanced by increasing the percentage of conducting nano-particles. In addition, it is possible to decrease the loss in a material by mixing low-loss dielectric nano-particles powder in a lossy material.**

***Index terms* — Alumina nano-particles, carbon nanotubes, composite material, microwave characterization, nanotechnology, percolation, permittivity measurements.**

I. Introduction

Materials in pulverized form are challenging to characterize due to the density-dependence of electrical properties and the presence of air gap between particles. However, it is a decisive step to understand and design novel materials for future radio frequency (RF) devices. The electrical characterization of composite material is particularly interesting for their new electrical properties [1]-[2]. Nelson [3] has described different models to estimate the complex permittivity of bulk material from its pulverized form. However, those models fail in the case of nano-particles as explained in [4] where it is observed the enhancement of the real part of the permittivity of composite nano-material. Also in [5], it is reported at low frequencies in the range of few MHz dramatic values of complex permittivity for carbon nanotube networks where percolation theory [6] is used to interpret the reason for high values for both real and imaginary parts of complex permittivity.

The objective of this work is to explore changing in a controlled manner the complex permittivity of nano-particles of alumina by mixing with carbon nanotubes. For this purpose, the complex effective permittivity of pure alumina nano-particles is obtained. Then, carbon nanotubes in a dry-powder form as furnished by the manufacturer are characterized. Finally, we show that by mixing alumina and CNT in a controlled approach, it is possible to synthesize a novel nano-composite material with interesting electrical properties which could have appealing RF applications.

II. Description of Test Structure

The measurement setup used in this work for material characterization consists mainly of a hollow circular waveguide shorted at one end to hold the pulverized material under test (MUT). This hollow cylinder corresponds to region IV shown in Fig. 1 (a) and it is connected to a 50-Ω air-filled coaxial transmission line that corresponds to region I through regions II and III which are air-filled coaxial transitions. The technique of complex permittivity extraction involves an iterative optimized gradient method where the simulated reflection coefficient is compared to the one obtained from microwave measurements using a performance network analyzer (PNA). In this inverse optimization problem, the effective complex permittivity ($\varepsilon_{\text{eff}} = \varepsilon'_{\text{eff}} - j\varepsilon''_{\text{eff}}$) of the material under test is the unknown optimization variable. The search for complex permittivity stops when the absolute difference between the measured and simulated reflection coefficients is less than 10^{-8}[19]. The simulation is based on full-wave modeling where coaxial and circular discontinuities are modeled using mode matching technique (MMT) [7]. Each discontinuity is characterized by its generalized scattering matrix (GSM) block. The different blocks of GSMs are connected in cascaded as shown in Fig. 1 (b) through transmission lines that represent the actual lengths of different regions. The final structure is modeled as a one-port network characterized by its reflection coefficient S_{11}. It is noted that full-wave analysis based on MMT accurately models the discontinuities in cascade encountered by an incident electromagnetic wave as it involves all propagating and evanescent modes of each region depicted in Fig. 1 (a).

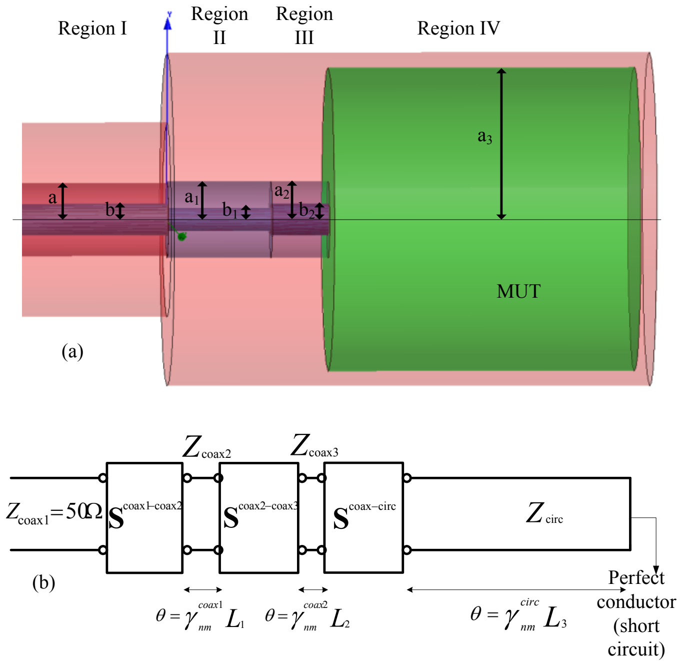

Fig. 1: (a) Schematic of the test structure. (b) Cascaded blocks of generalized scattering matrices. The dimensions of setup are: a = 1.2 mm, $b = b_2$ = 0.52 mm, $a_1 = a_2$ = 1.265 mm, b_1 = 0.4 mm, a_3 = 4.9 mm, L_1 = 3.4 mm, L_2 = 1.8 mm, L_3 = 10 mm.

(a) (b)

(c) (d)

Fig. 2: Actual picture of the different parts of fabricated test setup. (a) plunger. (b) Plunger support. (c) Coaxial lines of regions I to III. (d) Hollow circular waveguide, region IV. Part (a) goes into (b) on top of (d) to pack the powder inside (d), then removed. Measurements are realized when part (c) is ended with part (d) filled with powder.

The rigorous derivation of the mode matching technique-based model and convergence studies has been previously discussed in [7]. The results presented in [7] show that the permittivity has been successfully retrieved from reflection coefficient (S_{11}) with an error less than 2%. In addition, the extraction procedure has been applied to air as a lossless material and water as a lossy material. The results are in good agreement with other references found in the literature. In [11], the accuracy for the real part of the permittivity ε' less than 3% and the imaginary part with accuracy less than 5% was reported using an APC7mm connector when the loss tangent $\varepsilon''/\varepsilon'$ is greater than ±0.01, yet the frequency range was limited to 18 GHz.

In this work, the microwave measurements are done using PNA: Agilent E8361A. This PNA has a measurement range from 10 MHz up to 67 GHz. The output ports of this PNA are 1.85 mm connectors. To avoid any phase ambiguity due to calibration, the 50-Ω line of region I is machined with the same dimensions as those of a 2.4 mm male connector. In this case, the 1.85 mm cable is connected directly between the PNA and the testing cell without the need for any adapter in between. By reducing the size of the test cell and using a 2.4 mm precision adapter, we are able to carry measurements in the frequency range from 10 MHz to 50 GHz using a single test setup [7]. The fabrication tolerance of the micro-machined test setup as verified by optical methods is less than 10 µm.

III. Results and Discussions

The microwave measurements are carried out for pure alumina powder, carbon nanotubes, and a mixture of CNTs and alumina. The alumina used in this work is supplied by South Bay Technology, Inc. The nano particles of alumina have a diameter of 50 nm. The CNTs are provided by Bucky USA (product number BU-203) and they have a purity > 90 wt%, ash < 1.5 wt%, diameter 1 nm to 2 nm, and length 5 μm to 30 μm. For each material, nano-particles are weighted then dropped directly into the hollow-cylinder (region IV) holder. MUT is packed in the holder by exercising manual press through a plunger and a plunger support as shown in Fig. 2 (a) and (b), respectively, to progressively increase the density inside the holder shown in Fig. 2 (d). The volume of cavity V is determined using optical measurements and the weight M of MUT is obtained using analytical balance with ±0.01mg precision. The packing density is computed using the following relation: $\rho = \frac{M}{V}$.

A. Nano-Particles of Alumina

Dry powder of only nano-particles of alumina is used as furnished by the manufacturer. The average size of alumina particles is 50 nm. Fig. 3 shows the real and imaginary parts of the complex effective permittivity of pure alumina versus frequency at different packing densities.

Fig. 4 presents the variation of complex effective permittivity of alumina versus packing density and volume fraction at a frequency of 3 GHz. Volume fraction is defined as the ratio of the actual volume of nano particles to the total volume of container. In this case, alumina is weighed and the volume is obtained from $V_{act} = \frac{M}{\rho}$ where ρ = 3.9 g/cm^3 for alumina. The volume of holder cavity is 0.7854 cm^3. The linearly extrapolated results shown in Fig. 4 suggest that if a packing density equal to the bulk density of alumina is reached then the bulk permittivity of alumina is obtained. This linear variation of complex permittivity versus packing density is different from those models initially proposed in [3] for particles with sizes between 50-100 µm and discussed in [4] to extract bulk permittivity. The reason that initial models introduced in [3] fails for nano-particles is attributed to the reduction of air gaps between particles synthesizing a better homogeneous material as illustrated by the cartoon in Fig. 5 where particles are assumed to be spherical in shape. In other words, solid spheres corresponding to the alumina particles with larger radii leads to bigger voids between the particles which is equivalent to an air-alumina mixture and the effective permittivity of the mixed material is dominated by the air permittivity. As the radii of alumina particles decrease, voids between the solid spherical particles are reduced. As the size of interstices becomes smaller than the wavelength of the electromagnetic waves propagating in the material the alumina nano-particles can be considered quite a homogenous medium.

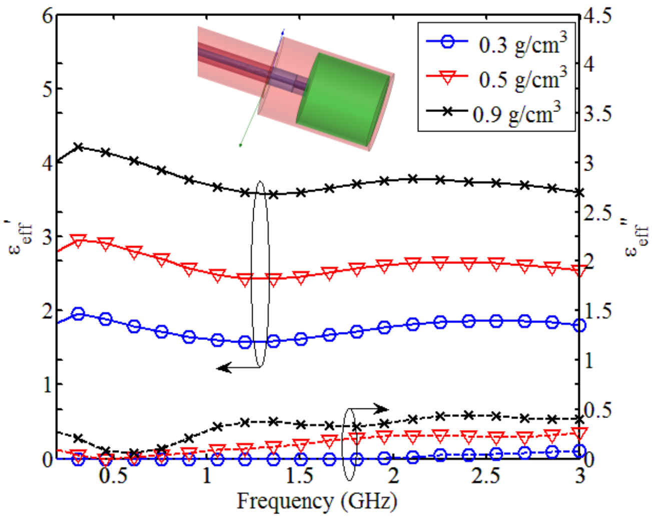

Fig. 3: Variation of the extracted complex effective permittivity of alumina versus frequency at different densities using the structure shown in the inset. The left axis corresponds to the real part of complex effective permittivity represented by solid lines while the right axis corresponds to the imaginary part shown by dashed lines. Same marker is used to represent both real and imaginary parts at each packing density.

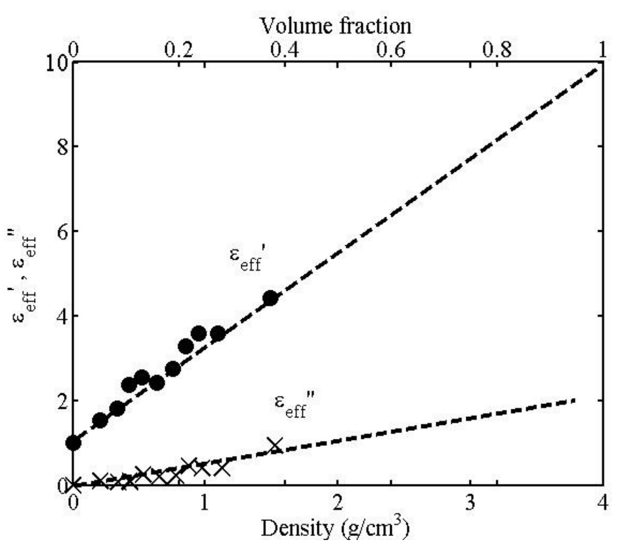

Fig. 4: Variation of extracted complex effective permittivity of alumina versus packing density or the volume fraction at 3 GHz. The straight dashed black lines represent a linear curve fitting of data. The same scale is used for the real ($\varepsilon'_{\text{eff}}$)and imaginary ($\varepsilon''_{\text{eff}}$) parts of the effective permittivity.

Meanwhile the size of air interstices between alumina nano-particles decreases, their number has significantly increased. It is reported in [9] that the losses are less sensitive for granular particles with size greater than 3-4 µm in a fully dense material. However, for this case study, the loss dependence is strongly influenced by the porosity of the alumina nano-particles. This explains why the extracted imaginary part of the complex effective permittivity shown in Fig. 4 is higher than the one obtained in [9] for sintered alumina.

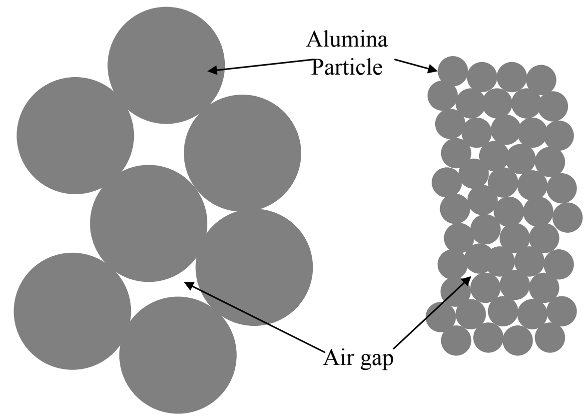

Fig. 5: Schematic of alumina particles explaining the dependence of material electrical properties on the size reduction of particles from 50-100µm (left-hand side) to 50nm (right-hand side). Dimensions are not to scale.

It should be noted that the packing density of alumina in the holder is progressively increased. Hence, the ratio of air to alumina is decreasing as the packing density is increased. For the particular scenario where packing density is 0, the holder is entirely empty, i.e., filled with air and the extracted permittivity corresponds to the case of air as shown in [19].

B. Carbon Nanotube Networks

CNTs are tested as supplied by manufacturer in their dry-powder form. Fig. 6 shows the complex effective permittivity at different packing densities.

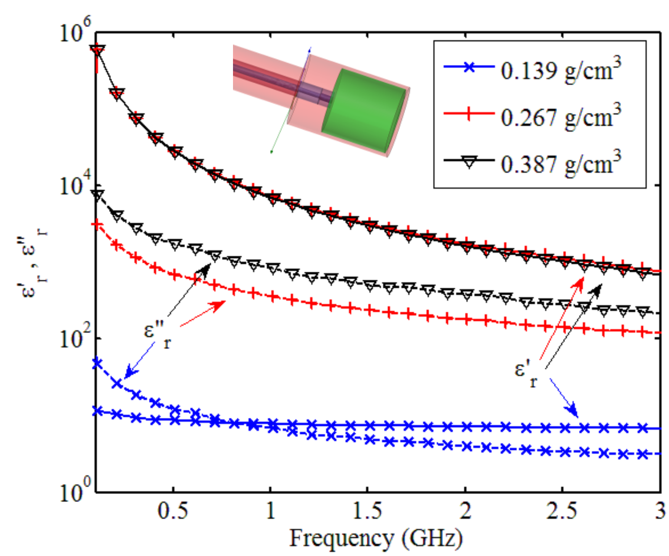

Fig. 6: Variation of the complex permittivity of carbon nanotube networks in a dry-powder form at different packing densities when the structure shown in the inset is filled with MUT. Different markers are assigned for each density. The solid lines represent the real part $\varepsilon'_{\text{eff}}$ of the permittivity while the dashed lines correspond to the imaginary part $\varepsilon''_{\text{eff}}$. Both real and imaginary parts have the same scale.

The effective permittivity is monotonically decreasing with frequency. It is observed that at low frequencies, the real and imaginary parts of the permittivity are the largest. The dramatic value of real and imaginary parts of complex permittivity obtained at lowest frequency and highest density are in agreement with those large values reported in [5], [12] and [17].

The effective complex permittivity is plotted in Fig. 7 versus packing density. The imaginary part of the permittivity ε'' is related to the conductivity of the CNTs: $\varepsilon'' = \frac{\sigma}{\omega\varepsilon_0}$ where ω is the angular frequency and $\varepsilon_0 = 8.85 \times 10^{-12}(\mathrm{F/m})$ is the vacuum permittivity. In the inset of Fig. 7, the real and imaginary part of the effective permittivity function of the density are plotted in log-log scale at 3 GHz to extract the relevant parameters of the percolation curves.

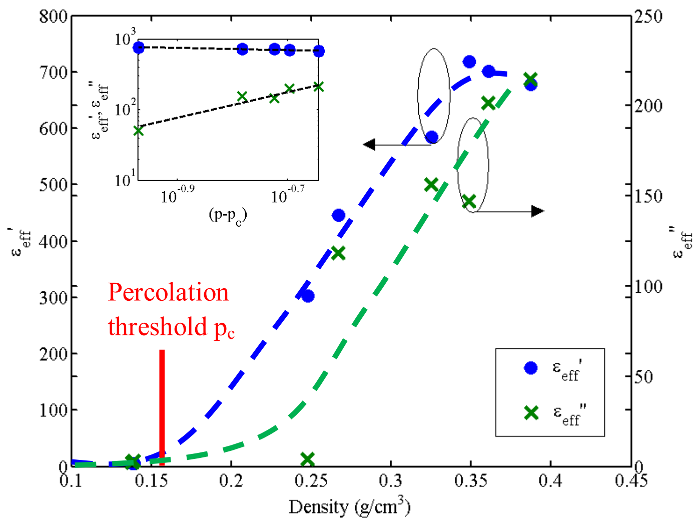

Fig. 7: Variation of the real (dot) and imaginary (cross) parts of the complex effective permittivity of carbon nanotube networks versus density at 3 GHz**.** The inset presents the log-log plots of the real and imaginary part of the complex effective permittivity functions of the occupation probability.The dashed lines in the inset are the means values fitting curves based on equation (1).

Above the percolation threshold p_c , the real and imaginary parts of the effective permittivity of a conductor-insulator mixture can be expressed in terms of a power law relation as follows:

$$\varepsilon', \varepsilon'' \propto (p - p_c)^t \text{ for } p > p_c \quad (1)$$

where p is the occupation probability and t is the critical exponent. It should be noted that the CNT networks include metallic nanotubes, semiconducting nanotubes, and air voids. Hence, the variable packing density is adopted in this work to describe the percolation behavior instead of the volume/weight fraction. The critical exponent t is usually between 1.6 and 2 in a three dimensions percolation networks. However, experiments show that its value varies from 1.3 to 3.1 [13]. In Fig. 7, the percolation threshold p_c corresponding to the packing density of 0.16 g/cm^3 represents the onset of material changing behavior from dielectric to conductive. For the studied CNTs, the critical exponent obtained by the linear regression fitting curve of the imaginary part of the effective permittivity shown in the inset of Fig. 7 is 1.8 at 3 GHz which agree with the percolation data reported in the literature. The region below percolation threshold where the dielectric constant increases rapidly has been studied experimentally and theoretically in [14]. Below percolation threshold, it is observed that the material behaves as an insulator a large dielectric constant and small losses. In this work, we study the nano-material characteristics above its percolation threshold where it behaves as a conductor. Thus, a saturation followed by decreasing of the real part of the permittivity versus packing density is observed while the imaginary part continuously increases as shown in Fig. 7. Applying (1) to the fitting curve of the real part of the permittivity shown in the inset of Fig. 7, gives a negative critical exponent (-0.15) due to the decrease of the dielectric constant. The fact that the dielectric constant decreases above percolation threshold with the increase of packing density is because the material under test becomes more conducting due to the increasing number of metallic nanotubes. Ultimately, the real part of the permittivity should theoretically reach 1 as for a metallic material.

It is noted that the CNT networks as produced by manufacturer consist of a 1:2 ratio where 1/3 of metallic nanotubes is mixed with 2/3 of semiconducting nanotubes [15]. At low frequencies, the interaction between metallic and semiconducting nanotubes enhances the real part of complex effective permittivity. In [4], the experimental measurements applied to a mixture of nano-particles of alumina and micro-particles of copper show the contribution of packing density and the composition of a mixture of metallic-dielectric nano particles to the large values of complex permittivity.

Moreover, studies in [1] and [16] suggest that the nonlinear-behavior of permittivity can be enhanced by changing the aspect ratio of mixed nano-particles**.** At low frequencies, the interaction between metallic and semiconducting nanotubes enhances the real part of complex effective permittivity. In [4], the experimental measurements applied to a mixture of nano-particles of alumina and micro-particles of copper show the contribution of packing density and the composition of a mixture of metallic-dielectric nano particles to high values of complex permittivity. Two-physical mechanisms may explain this permittivity enhancement [5] and [18]. First, electrical field creates a surface charge polarization on the interface between metallic and dielectric particles which yields an increase in capacitance. Second, dipole polarization contributes to global permittivity when the frequency of applied electrical field is lower than the relaxation frequency of metallic particles.

In Fig. 8, the locus in the complex plane of the relative complex permittivity divided by bulk density for carbon nanotube networks can be used to predict the behavior of the material.

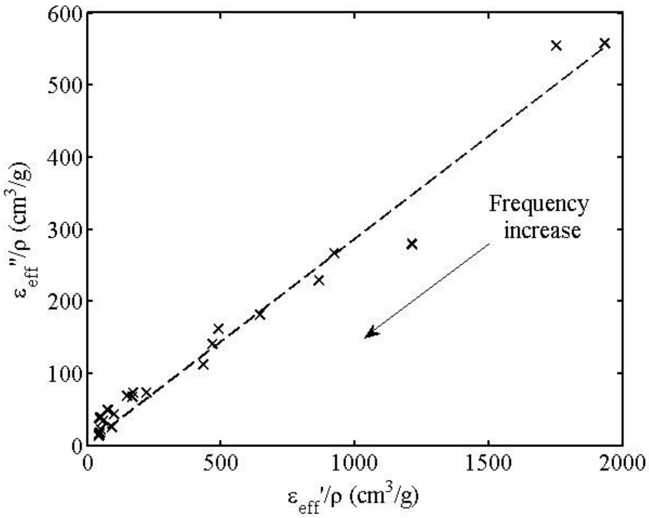

Fig. 8: Locus in the complex plane of the relative complex permittivity divided by bulk density for carbon nanotube networks. The black dashed line represents the linear approximation of the extracted data using the measurements setup as presented in the inset.

C. *Mixture of Alumina and Carbon Nanotubes*

This section is dedicated to the extraction of the complex permittivity of CNT-based composite materials. The CNT-based composite material is realized by mixing 1g of alumina with 0.2g of CNT. Transmission electron microscopy (TEM) of prepared mixture is shown in Fig. 9.

Another procedure used to characterize the mixture is the Energy-dispersive X-ray spectroscopy (EDX) shown in the inset of Fig. 9. The EDX where three peaks can be distinguished is representative of the mixture sample realized at different positions in the sample. The first peak indicates the presence of carbon due to CNTs as well as the carbon grid used to deposit the samples explaining the high magnitude compared to other components. The second and third peaks indicate the presence of oxygen and aluminum due to alumina particles (Al_2O_3).

Based on our previous studies [5], [17], [19] as well as the work reported here, the extracted complex permittivity of CNT networks is significantly large at low frequencies as shown in Fig. 6 and drops by several orders of magnitude at higher frequencies. This trend is observed independent of the packing density. At higher frequencies, both real and imaginary parts of the effective permittivity converge to asymptotic values corresponding to bulk material. As we anticipate that the main effect due to the addition of CNTs in alumina medium occurs at low frequencies, we have limited the maximum measurement frequency to 3 GHz.

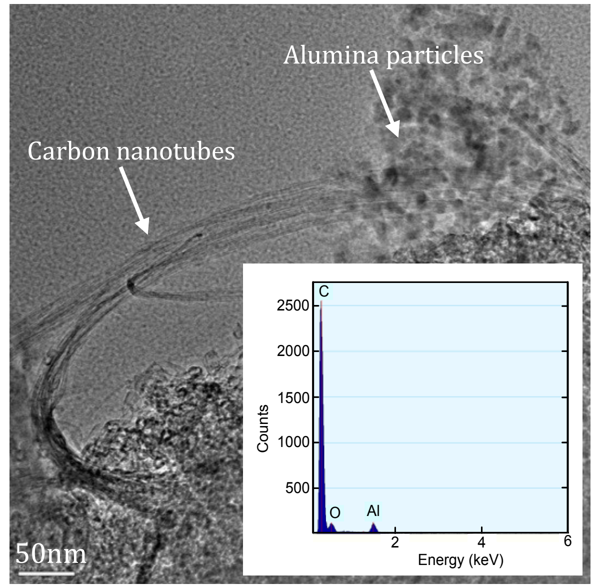

Fig. 9: TEM picture of the prepared mixture of alumina and carbon nanotubes. The inset is the EDX showing the different particle components found in the sample.

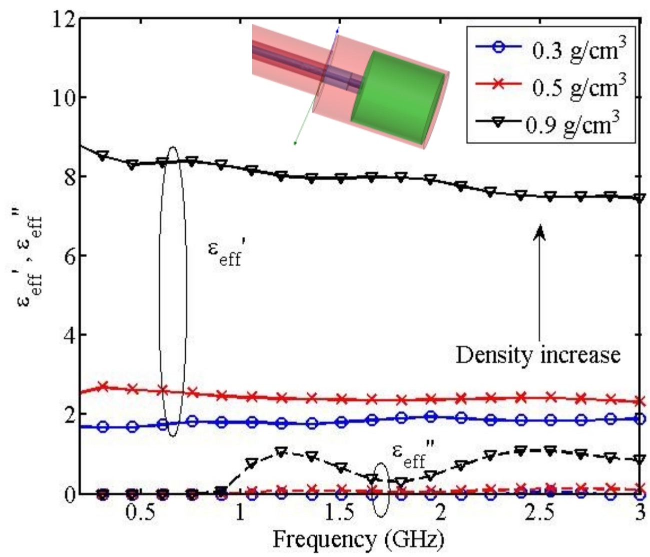

Fig. 10: Variation of the complex effective permittivity of a dry mixture of alumina and CNTs. The same marker is used for real and imaginary parts at each packing density. The same scale is used for the real (ε'_{eff})and imaginary (ε''_{eff}) parts of the effective permittivity.

The complex permittivity of the composite mixture versus frequency from 10 MHz to 3 GHz at different packing densities is presented in Fig. 10. Fig. 11 shows the variation of the complex permittivity of a dry mixture of CNTs and alumina versus density at a frequency of 3 GHz. In this figure, the data obtained for pure alumina are also plotted to highlight the increase of dielectric constant due to the mixing with CNTs.

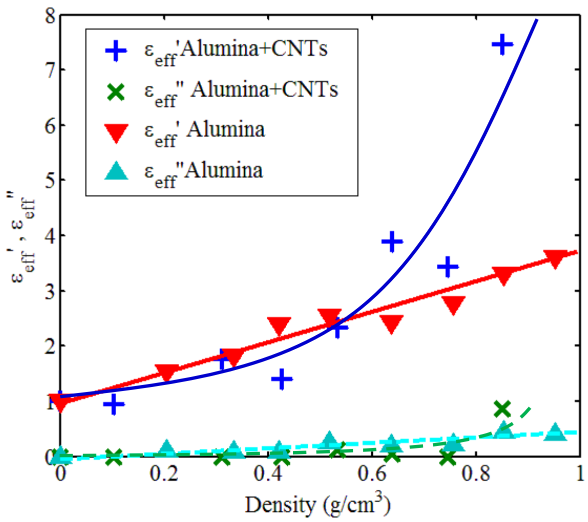

Fig. 11: Variation of the real (solid line) and imaginary (dashed line) parts of the complex effective permittivity of a mixture of CNTs and alumina versus density. The data obtained for pure alumina are plotted to highlight the increase of dielectric constant of the composite material. Both real ($\varepsilon'_{\mathrm{eff}}$) and imaginary ($\varepsilon''_{\mathrm{eff}}$) parts of the effective permittivity are plotted on the same scale.

Fig. 12 summarizes the loss tangent of all nanomaterials characterized in this work.

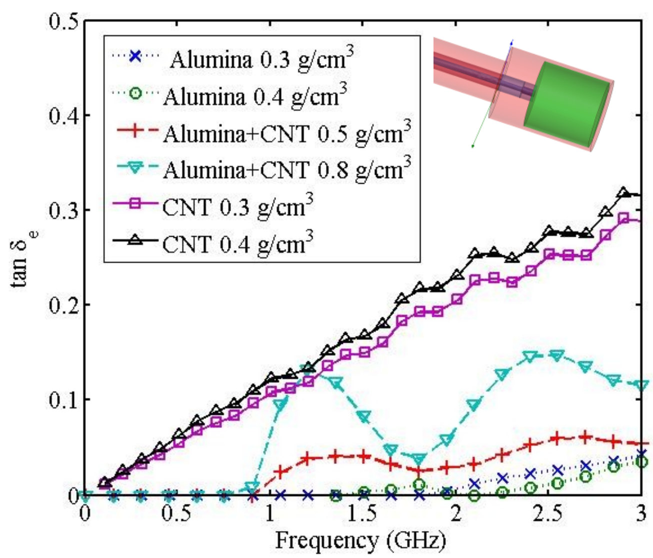

Fig. 12: Comparison of the loss tangent obtained for all nanomaterials characterized in this work considering different packing densities: alumina is shown by dotted lines, alumina mixed with carbon nanotubes by dashed lines and pure CNT powder by solid lines.

For each material the loss tangent increases with the packing density. Alumina well known as a low loss material is used as a reference as shown by dotted lines in Fig. 12. CNTs on the other hand have a high loss tangent as described by the solid lines in Fig. 12. By combining the electrical properties of alumina and carbon nanotubes, it is possible to obtain high values of dielectric constant controlled by CNTs as shown in Fig. 11 and low loss tangent controlled by alumina as shown in Fig. 12.

IV. Radio frequency (RF) applications

The characterization of the electrical properties of nano-composites is necessary to understand and design novel material for high-frequency applications. For instance, initial work was carried out in [5] to explore the potential of replacing metallic traces with CNT for interconnect applications. For this purpose equivalent circuit models of those interconnect were developed in [20]-[21]. Dielectric resonators used in microwave/RF circuits require a high-dielectric constant and or low loss to achieve high quality factor. In addition, the resonant frequency is inversely proportional to the square root of the real part of the permittivity and the dimensions of resonator. Consequently, at low frequencies, dielectric resonators are not used mainly due to their large size. Earlier work by El Sabbagh [22] shows the possibility of building a CNT-based miniaturized resonator.

In Section III, we showed that the mixing of CNTs with alumina significantly enhances the real part of permittivity without increasing the losses represented by the imaginary part of the permittivity as shown in Fig. 12. These results are in agreement with those in [22] confirming the role of CNT to miniaturize RF resonators. Other researchers have shown that above percolation threshold, a multi-conducting path through the CNT-based composite material can be used to tune the electrical properties of the medium [23] by introducing a small bias voltage across the composite material. This is another interesting application in tunable circuits. Moreover, CNTs composite materials were studied in [24] for electromagnetic interference (EMI) shielding to protect delicate electronic devices against external electromagnetic radiation. In the last decade, high-k gate dielectric appeared in semiconductor technology and progressively replaced silicon dioxide insulator layers to further miniaturize microelectronic components without sacrificing the performance of CMOS transistors at high frequency [25]. Our work shows that CNT-based composites may be a possible candidate as future high-k gate dielectric implemented in high-frequency silicon-based transistors.

Several research groups have demonstrated the RF applications in radio systems where carbon nanotubes detect an amplitude modulation (AM) signal in a functioning radio receiver as replacement of diode in current radio systems [26]-[27]. CNTs are also among the possible candidates to implement future high frequency transistors due to their quasi-ballistic electron transport and their high intrinsic cut-off frequencies (up to terahertz). The main challenge is to control the alignment and the deposition of CNTs to form a semiconducting channel between the drain and source. Several alignment techniques have been investigated such as droplet, dielectrophoresis, Langmuir-Blodgett, spin coating and chemical vapor deposition (CVD) methods [28]; however, fabrication of CNT-field effect transistor (CNT-FET) on a large scale integration still needs to be improved to be competitive compared to traditional silicon based FET.

V. Conclusions

A measurement approach is presented to extract the complex effective permittivity of nano-particles pulverized materials considering the effect of packing density. The technique is applied to nano-particles of pure alumina, carbon nanotubes, and to a mixture of alumina and carbon nanotubes. For alumina, the linear dependence of complex effective permittivity on packing density gives an estimate of the permittivity of bulk material. The dramatic values of the real and imaginary part of the complex permittivity of CNTs at low frequencies are due to the interaction of metallic and dielectric nano-particles. The nonlinear behavior of the variation of the permittivity as a function of the packing density is experimentally demonstrated for a mixture of carbon nanotubes and alumina. The possibility to engineer CNT-based composites material with a high-dielectric constant and low loss has been shown. The compositions as well as the dispersion of the carbon nanotubes in a dielectric medium will be the key to engineer those new microwave composite materials.

ACKNOWLEDGMENTS

The authors thank D. Rogers for the fabrication of the test structure and M. Benamara for his expertise about the preparation of SEM/TEM samples. This research was sponsored by the Army Research Laboratory and was accomplished under Cooperative Agreement Number W911NF-10-2-0072. The views and conclusions contained in this document are those of the authors and should not be interpreted as representing the official policies, either expressed or implied, of the Army Research Laboratory or the U.S. Government. The U.S. Government is authorized to reproduce and distribute reprints for Government purposes notwithstanding any copyright notation herein.

REFERENCES

[1] N. Guo, S.A. DiBenedetto, P. Tewari, M.T. Lanagan, M.A. Ratner, T.J. Marks, "Nanoparticle, size, shape, and interfacial effects on leakage current density, permittivity, and breakdown strength of metal oxide-polyolefin nanocomposites: experiment and theory", Chem. Mater. 2010, 22, 1567–1578 1567.

[2] D. Gerbson, F. P. Calame, A. Bimboim, "Complex permittivity measurements and mixings laws of alumina composites," J. Phys. D: Appl. Phys vol.89, n.12, 15 June 2001.

[3] S.O Nelson, "Estimation of permittivities of solids from measurements on pulverized or granular materials," in Dielectric Properties of Heterogeneous Materials, A. Priou, Ed. New York: Elsevier, 1992, vol. 6, ch.6.

[4] E. Decrossas, M.A. EL Sabbagh, H.A., Naseem, V. Fouad Hanna, and S.M. El-Ghazaly, "Effective permittivity extraction of dielectric nano-powder and nano-composite materials: effects of packing densities and mixture compositions," in *IEEE European Microwave Conference*, Manchester, UK, 9-14 Oct. 2011.

[5] M.A. EL Sabbagh, S.M. El-Ghazaly, and H.A. Naseem, "Carbon nanotube-based planar transmission lines," *in IEEE MTT-S Int. Microwave Symp. Dig.*, Boston, MA, 7-12 June 2009, pp. 353-356.

[6] D.Stauffer and A.Aharony, *Introduction to Percolation Theory,* Taylor and Francis, Washington, DC, 1992.

[7] E. Decrossas, M.A. EL Sabbagh, V. Fouad Hanna and S.M. El-Ghazaly, "Mode Matching Technique based modeling of coaxial and circular waveguide discontinuities for material characterization purposes," *EuMA, International Journal of Microwave and Wireless Technologies,* Published online Sep. 28, 2011.

[8] T.J. Fiske, H.S. Gokturk, D.M. Kaylon, "Percolation in magnetic composites," J. Mat. Sci, 1997, vol.32, 5551-5560

[9] S. J. Penn, N. Mc.Alford, A. Templeton, X. Wang, M. Xu, M. Reece, and K. Schrapel, ''Effect of Porosity and Grain Size on the Microwave Dielectric Properties of Sintered Alumina,'' J. Am. Ceram. Soc., 1997, vol. 80 n. 7, pp.1885–1888.

[10] N.-E. Belhadj-Tahar, and A. Fourrier-Lamer, "Broad-Band Analysis of a Coaxial Discontinuity Used for Dielectric Measurements," *Microwave Theory and Techniques, IEEE Transactions on*, vol.34, no.3, pp. 346- 350, Mar 1986.

[11] N.-E. Belhadj-Tahar, O. Meyer, and A. Fourrier-Lamer, "Broad-Band Microwave Characterization of Bilayered Materials Using a Coaxial Discontinuity with Applications for Thin Conductive Films for Microelectronics and Material in Air-Tight Cell'" *Microwave Theory and Techniques*, *IEEE Transactions on*, vol. 45, no, 2, pp. 260-267, Feb. 1997.

[12] H. Xu, M. Anlage, L. Hu, and G. Gruner, "Microwave shielding of transparent and conducting single-walled carbon nanotube films," *in J. Appl. Phys.* Vol. 90, 183119, May 2007.

[13] N.K. Shrivastava, B.B. Khatua, "Development of electrical conductivity with minimum possible percolation threshold in multi-wall carbon nanotube/polystyrene composites," in Carbon, vol. 49, no. 13, pp. 4571-4579, 2011.

[14] L. Wang, Z.M. Dang, "Carbon nanotube composites with high dielectric constant at low percolation threshold," in Appl. Phys. Lett., vol. 87, 042903, 2005.

[15] M. S. Dresselhaus, G. Dresselhaus, and P. Avouris, *Carbon Nanotubes Synthesis, Structure, Properties and Applications*. Springer-Verlag, Berlin, 2001.

[16] S. Link, M.B. Mohamed, and M.A. El-Sayed, "Simulation of the optical Absorption spectra of gold nanorods as a function of their aspect ratio and the effect of the medium dielectric constant," J. Phys. Chem. B 1999, 103, pp. 3073-3077.

[17] E. Decrossas, M.A. EL Sabbagh, V. Fouad Hanna and S.M. El-Ghazaly, "Broadband characterization of Carbon nanotube networks," in *IEEE Int. Symp. Electromagnetic Compatibility*, Fort Lauderdale, FL, 27–30. 2010, pp. 208–211.

[18] R. Ravindran, K. Gangopadhyay, S. Gangopadhyay, N. Mehta and N.Biswas, "Permittivity enhancement of aluminum oxide thin films with the addition of silver nanoparticles," 2006 J. Phys. D: Appl. Phys. 89, 263511.

[19] E. Decrossas, M.A. EL Sabbagh, V. Fouad Hanna and S.M. El-Ghazaly, "Rigorous characterization of carbon nanotube complex permittivity over a broadband of RF frequencies," accepted for publication in *IEEE Transactions on Electromagnetic compatibility*.

[20] M.A. EL Sabbagh and S.M. El-Ghazaly, "Frequency-Dependent Circuit Models of Carbon Nanotube Networks," in *IEEE 18th Conference on Electrical Performance of Electronic Packing and Systems*, Portland, OR, pp. 129–132, 19-21 Oct. 2009.

[21] M.A. EL Sabbagh and S.M. El-Ghazaly,"Measurement-Based Models of Carbon Nanotube Networks," in *IEEE Radio and Wireless Symposium (RWS)*, New Orleans, LA, pp. 340–343, 10-14 Jan. 2010.

[22] M.A. EL Sabbagh and S. M. El-Ghazaly, "Miniaturized carbon nanotube-based RF resonator," in *IEEE MTT-S Int. Microwave Symp. Dig.*, Boston, MA, pp. 829-832, 2009.

[23] L. Liu, L.B. Kong, and S. Matitsine, "Tunable effective permittivity of carbon nanotubes composites," in Applied Physics Letters, vol. 93, 113106 (2008).

[24] N. Li, Y. Huang, F. Du, X. He, Xi. Lin, H. Gao, Y. Ma, F. Li, Y. Chen, and P.C. Eklund, "Electromagnetic interference (EMI) shielding of single-walled carbon nanotube epoxy composites," in Nano lett., 2006, vol. 6, no. 6, pp. 1141-1145.

[25] D. Barlage, R. Arghavani, G. Dewey, M. Doczy, B. Doyle, J. Kavalieros, A. Murthy, B. Roberds, P. Stokley, and R. Chau, "High-frequency response of 100nm integrated CMOS transistors with high-K gate dielectrics', in *Electron Devices Meeting, 2001. IEDM Technical Digest. International*, Washington, DC, USA, pp.10.6.1-10.6.4.

[26] C. Rutherglen, and P. Burke, "Carbon nanotube radio," in *Nano Lett.*, vol. 7, pp. 3296–3299, 2007.

[27] K. Jensen, J. Weldon, H. Garcia, and A. Zettl, “Nanotube radio,” in *Nano Lett.*, vol. 7, pp. 3508–3511, 2007.
[28] C. Rutherglen, D. Jain, and P. Burke, “Nanotube electronics for radiofrequency applications’, in *Nature nanotechnology*, vol. 4, pp. 811-819, 2009.

Emmanuel Decrossas (S’10) received the B.S. and M.S with honors in engineering science and electrical engineering from the université Pierre et Marie Curie Paris-6, Paris, France in 2004 and 2006 respectively. He is actually pursuing his Ph.D. in electrical engineering in the University of Arkansas, Fayetteville, AR, USA. In 2004, he joined France Telecom for an internship to develop and update the intranet services. He was an intern in Laboratoire de Génie Eléctrique de Paris (LGEP) in 2005. Mr. Decrossas was a visiting scholar student in 2006 in the University of Tennessee to initiate an international student exchange program and work on reconfigurable MEMS antennas for wireless applications. His research interests include dielectric characterization, computer-aided design of microwave devices, micro-fabrication and nanotechnology to fabricate and model high frequency devices.
Mr. Decrossas is member of the electrical engineering honor society Eta Kappa Nu and has been cited in the who's who among students in American universities & colleges in recognition of outstanding merit and accomplishment as a student at the University of Arkansas Fayetteville in 2011.

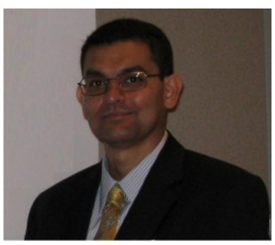

Mahmoud A. EL Sabbagh (S’93–M’02–SM’06) received the B.S. (with honors) and M.S. degrees in electrical engineering from Ain Shams university, Cairo, Egypt, in 1994 and 1997, respectively, and the Ph.D. degree from the University of Maryland, College Park (UMCP), in 2002.
Dr. Sabbagh is holding the position of Professor of Practice in the EECS Department, Syracuse University and also working with Anaren Microwave, Inc. He is cofounder of EMWaveDev where he is involved in the design of ultra-wideband microwave components. Dr. EL Sabbagh is a senior member of IEEE, received Ph.D. degree from the University of Maryland College Park, College Park, MD in 2002. He worked at several academic and governmental institutes in Cairo, Canada, and US..His research interests include computer-aided design of microwave devices, microwave filter modeling and design for radar and satellites applications, dielectric characterization, metamaterial, EM theory, and RF Nanotechnology. Prof. EL Sabbagh is a member of Sigma Xi and he was cited in the 2008–2009 edition of “Who’s Who in Science and Engineering.”

Victor Fouad Hanna (F’96) received the B.Sc degree (honors) in electronics engineering from Cairo University, Cairo, Egypt in 1965, and the M.Sc. degree in microwave engineering from Alexandria University, Egypt in 1969. He received the D.Sc. degree [Doctorat -Sciences Physiques (doctorat d’Etat)] from l’Institut National Polytechnique (I.N.P.), Toulouse, France in 1975.
Since 1997, he is a professor at the University Pierre et Marie Curie (University of Paris 6) in the electronic department. His current research interests deal with electromagnetic theory, numerical methods for solving field problems, millimeter-wave transmission lines and bio-electromagnetism.
Prof. Fouad Hanna was selected as recipient of the IEEE third Millenium medal. He was the president of the IEEE France Section during the period 2002-2005. He is a member of the Region 8 IEEE Educational Activities Committee since January 2003 and a chair of this committee for 2004, 2005 and 2006. He is chair of the region 8 Awards and Recognition Committee since January 2007. Prof. Fouad Hanna was an elected member of the IEEE Fellow Committee for the years 2008 and 2009.

Samir M. El-Ghazaly (S’84–M’86–SM’91–F’01) received the B.S and M.S with honors in electronics and communications engineering from Cairo university in 1981 and 1984, respectively and the Ph.D. degree in electrical engineering from the University of Texas at Austin, in 1988.
He is currently the department head of the University of Arkansas, Fayetteville, since 2007. His research interests include RF and microwave and millimeter-wave semiconductor devices, electromagnetic, and numerical techniques applied to MMICs radio-frequency nanotechnology devices.
Prof. El-Ghazaly is a member of Tau Beta Pi, Sigma Xi, and Eta Kappa Nu. He is an elected member of Commissions A and D, URSI. He is a member of the Technical Program Committee for the IEEE Microwave Theory and Techniques Society (IEEE MTT-S) International Microwave Symposium (IMS) since 1991. He is on the Editorial Board of the IEEE kTRANSACTIONS ON MICROWAVE THEORY AND TECHNIQUES. He is an elected member of the Administrative Committee of the IEEE MTT-S. He is the editor-in-chief of the IEEE MICROWAVE AND WIRELESS COMPONENTS LETTERS. Prof. El-Ghazaly was the president of the IEEE's Microwave Theory and Techniques Society (MTT-S) in 2010.